

METHODS OF RADIATION EFFECTS EVALUATION OF SiC/SiC COMPOSITE AND SiC FIBERS - G. E. Youngblood and R. H. Jones (Pacific Northwest National Laboratory)*

OBJECTIVE

The objective of this work is to examine current practice for comparing the mechanical and thermal properties of irradiated, continuous SiC fiber/SiC matrix composites (SiC/SiC) and SiC fibers.

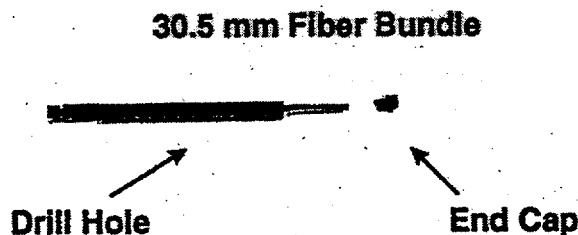
SUMMARY

This report covers material presented at the IEA/Jupiter Joint International Workshop on SiC/SiC Composites for Fusion Structural Applications held in conjunction with ICFRM-8, Sendai, Japan, Oct. 23-24, 1997. Several methods for radiation effects evaluation of SiC fibers and fiber-reinforced SiC/SiC composite are presented.

PROGRESS AND STATUS

Fiber Irradiations

Figure 1 illustrates a SiC fiber bundle contained within a SiC tube holder that is ideal for protection of the fiber bundle during high temperature irradiations. The tube holder, 2 mm od x 1 mm id and typically measuring from 30 to 60 mm in length, is made from sintered Hexoloy™ SiC. Placement and arrangement of the small drill hole(s) along the tube holder serve to identify the enclosed fiber bundle type and to allow gas exchange during encapsulation or during irradiation. The sintered SiC tube also can serve as a passive SiC temperature monitor [1].



Sintered Hexoloy™ SiC Fiber Tube Holder

Figure 1. A SiC fiber bundle loaded into a capped Hexoloy SiC tube for irradiation tests at high temperature and dose. This holder is 33.5 mm x 2 mm o.d. x 1 mm i.d.

*Pacific Northwest National Laboratory is operated for the U.S. Department of Energy by Battelle Memorial Institute under Contract DE-AC06-76RLO 1830.

Figure 2 illustrates how the length change of an irradiated fiber bundle can be determined. After irradiation, the fiber bundle is carefully pushed out of the SiC tube holder (Fig. 1) with a small diameter rod and laid on top of a graduated scale. Each fiber bundle end together with the reference scale is imaged through a microscope at about $\times 6$ magnification with a video camera. Digital images are stored in a video recorder for later analysis. In Fig. 2a, the fiber bundle ends were well-defined and the length was determined to the nearest 0.01 inch. In Fig. 2b, the fiber bundle had shrunk considerably, and the bundle length was determined to the nearest 0.05 inches due to the ill-defined ends.

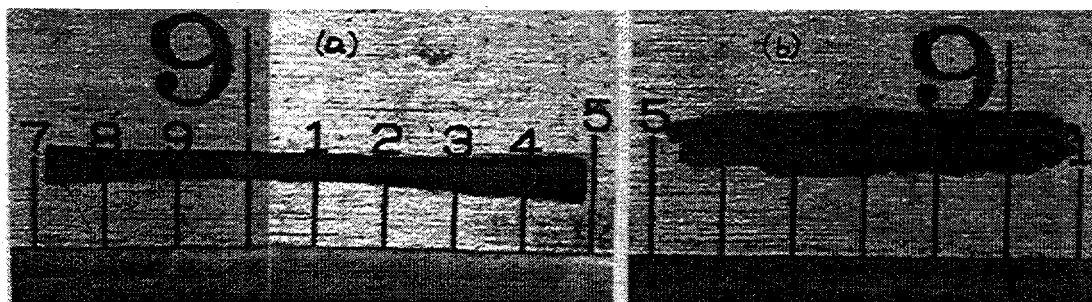


Figure 2. Examples of length change measurements for irradiated fiber bundles. The unirradiated fiber bundle lengths originally were 0.80 ± 0.01 inches; the uncoated Nicalon CG bundle (left) shrunk $3.9 \pm 0.3\%$; the pyrocarbon-coated Tyranno bundle (right) shrunk $32 \pm 1\%$.

Fiber Density

Figure 3 illustrates how the density of a fiber bundle is determined using the liquid gradient column technique. The column is constructed to cover a working range of densities of about 0.4 g/cc by using appropriate mixtures of carbon tetrachloride (1.594 g/cc), bromoform (2.890 g/cc) and methylene iodide (3.325 g/cc). At least five calibrated glass floats are used as density references for each column. The figure shows a typical 1 cm long sample cut from an irradiated fiber bundle suspended at 23.20 ± 0.02 cm and one of the calibration balls at ≈ 19 cm. For this column, each centimeter is equivalent to a change in density of about 0.003 g/cc, which represents the typical precision for these fiber density measurements.

Using these two techniques, a comparison of relative density and length changes for irradiated coated and uncoated SiC-based fibers is given in Table 1, Reference [2] of this report. From the density and length changes, fiber mass losses were calculated. The mass losses (also given in Table 1) predicted for the irradiated pyrocarbon-coated Tyranno and Nicalon CG fibers were significant, while the uncoated fibers appeared to exhibit no mass loss.

Overall irradiated fiber stability is indicated by examining the fiber density as a function of dose. As an example, the densities for four categories of SiC fibers (uncoated) irradiated up to 70×10^{25} n/m² (≈ 80 dpa-SiC) also are given in [2].

Fiber Crystallite Size

Long-term SiC fiber strength degradation occurs primarily due to extensive crystallization and crystal-growth in the fiber during high temperature, high dose irradiations. SEM images of

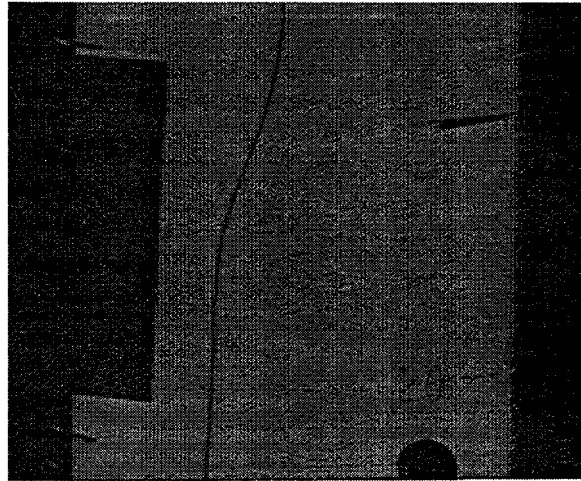


Figure 3. Typical view of a suspended SiC fiber bundle in a liquid density gradient column.

irradiated fiber surfaces depicting crystal growth are given in Figure 1 of Reference 2. Bulk fiber crystallite growth was determined by a modified Scherrer XRD technique. Table 1 presents the procedural changes from the conventional XRD technique necessary to accommodate relatively short (about 2.5 cm) irradiated fiber bundle segments. To achieve acceptable XRD peak resolution from a 5 mg sample, the background signal was reduced by using a silicon wafer substrate, the ground irradiated fibers were contained in 3-in-1 oil, the scan rate was reduced to 0.0002 °/sec, and the 2θ scan was reduced to the 25-50° range to cover only the β -SiC $\langle 111 \rangle$ peak and the $\langle 200 \rangle$ shoulder.

Table 1. Crystallite size of irradiated SiC fibers by a modified Scherrer XRD technique.

Procedure	Conventional	Irradiated
Sample Quantity	50 mg (\approx 25 cm tow)	5 mg (\approx 2.5 cm tow)
Substrate	Quartz	$\langle 100 \rangle$ Silicon
Containment	Colloidon	3-in-1 Oil
Range 2θ	10°-120°	25°-50°
Scan Rate	0.02 °/sec (\approx 1.5 hr.)	0.0002 °/sec (\approx 1.5 day)

Using these modified XRD procedures, the crystallite sizes for Hi Nicalon and Nicalon CG fibers were determined to have increased after a 800°C, 80 dpa-SiC irradiation (COBRA 1A2) from 2.7 to 6.1 nm and from 1.6 to 4.0 nm, respectively.

Fiber Creep

In References 3,4 and 5, an experiment developed to examine the creep behavior of irradiated SiC fibers by a bend stress relaxation technique is described, so will not be discussed here.

SiC/SiC Composite Mechanical Properties

To evaluate the radiation effects in SiC/SiC composite, the 4-point flexure test provides an easily reproduced standard method (See Reference 6 for recommended flexure test procedures). It is noted here that simple weighing of bend bars before and after irradiation

provides additional information about the material thermochemical stability, which can be quite different from that observed in a non-irradiation environment. For instance, bend strength degradation was related to a mass-loss mechanism for five types of SiC/SiC composite irradiated in the COBRA 1A2 test series [7].

SiC/SiC Composite Thermal Diffusivity

The measurement of the thermal diffusivity by the laser flash technique is another reproducible standard method used to evaluate irradiation effects in SiC/SiC composite as well as in monolithic SiC. Usually for analysis, the measured thermal diffusivity (α) is converted to thermal conductivity (k) through the relation $k = \alpha \rho c_p$, where ρ and c_p are the bulk density and specific heat capacity at constant pressure, respectively. The bulk density is easily measured before and after irradiation and its temperature dependence is easily estimated. In contrast, because of the difficulty of making accurate heat capacity measurements especially as a function of temperature, the heat capacity term is not so easily estimated. Generally, the rule of mixtures and handbook values are used to calculate an effective heat capacity. Then, the assumption usually is made that the heat capacity term doesn't change during irradiation. However for fundamental analysis of the effects of irradiation, i.e., defect configurations, concentrations, thermal annealing behavior, etc., it is better to analyze the temperature dependence of α (or $1/\alpha$) rather than k since α is directly proportional to the phonon mean free path (see Fig. 4) and does not depend on a heat capacity estimate [8]. A detailed analyses of irradiation defect configurations and their annealing kinetics is planned for high-purity, Morton CVD β -SiC to be irradiated in the Jupiter P3-4 test series.

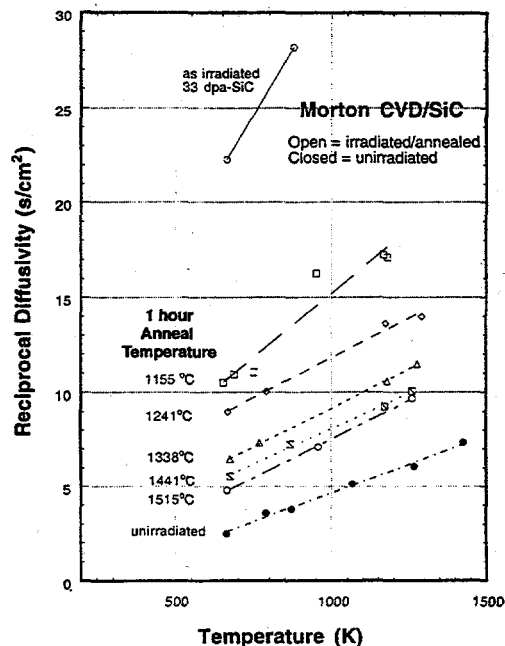


Figure 4. A plot of $1/\alpha$ vs. test temperature is approximately linear for unirradiated and for irradiated and annealed Morton CVD β -SiC. The intercepts are proportional to the residual irradiation defect concentrations after each high temperature anneal, and the approximately constant slopes represent the scattering strengths of the dominant phonon scattering defects, probably vacancies.

Nevertheless, for engineering application it is useful to analyze the temperature dependence of (K_{irr}/K_{unirr}), the ratio of the irradiated to the unirradiated thermal conductivity values, as was reported in [9] for a variety of monolithic and composite SiC structural materials.

REFERENCES

1. G. E. Youngblood, "Passive SiC Irradiation Temperature Monitor," p. 324 in Fusion Materials Semiannual Progress Report for Period Ending December 31, 1995. DOE/ER--0313/19.
2. G. E. Youngblood, R. H. Jones, Akira Kohyama and L. L. Snead, "Radiation Response of SiC-Based Fibers," extended abstract for paper P2-C111 presented at ICFRM-8, Oct. 26-31, 1997, Sendai, Japan (in this report).
3. G. E. Youngblood, M. L. Hamilton and R. H. Jones, "Technique for Measuring Irradiation Creep in Polycrystalline SiC Fibers," p. 146 in Fusion Materials Semiannual Progress Report for Period Ending June 30, 1996. DOE/ER--0313/20.
4. G. E. Youngblood and R. H. Jones, "Creep Behavior for Advanced Polycrystalline SiC Fibers," p. 89 in Fusion Materials Semiannual Progress Report for Period Ending December 31, 1996. DOE/ER--0313/21.
5. G. E. Youngblood, R. H. Jones G. N. Morscher and Akira Kohyama, "Creep Behavior for Advanced Polycrystalline SiC Fibers - II," p. 81 in Fusion Materials Semiannual Progress Report for Period Ending June 30, 1997. DOE/ER--0313/22.
6. G. E. Youngblood and R. H. Jones, "Minimum Bar Size for Flexure Testing on Irradiated SiC/SiC Composite," (in this report).
7. G. E. Youngblood, C. H. Henager and R. H. Jones, "Thermochemical Instability Effects in SiC-Based fibers and SiC/SiC Composites," p. 111 in Fusion Materials Semiannual Progress Report for Period Ending June 30, 1997. DOE/ER--0313/22.
8. G. E. Youngblood and W. Kowbel, "Improvement of the Thermal Conductivity of SiC/SiC Composite," p. 107 in Fusion Materials Semiannual Progress Report for Period Ending December 31, 1995. DOE/ER--0313/19.
9. G. E. Youngblood and D. J. Senor, "Analysis of Neutron Irradiation Effects on Thermal Conductivity of SiC-Based Composites and Monolithic Ceramics," p. 75 in Fusion Materials Semiannual Progress Report for Period Ending June 30, 1997. DOE/ER--0313/22.